

## Article

# Analysis of the IMERG-GPM Precipitation Product Analysis in Brazilian Midwestern Basins Considering Different Time and Spatial Scales

Luíza Virgínia Duarte <sup>1,\*</sup>, Klebber Teodomiro Martins Formiga <sup>2</sup>  and Veber Afonso Figueiredo Costa <sup>1</sup> 

<sup>1</sup> Environmental, Sanitation and Water Resources Postgraduate Program-SMARH, School of Engineering, Federal University of Minas Gerais, Belo Horizonte 31270-901, MG, Brazil

<sup>2</sup> Environmental and Sanitary Engineering Postgraduate Program-PPGEAS, School of Civil and Environment Engineering, Federal University of Goiás, Goiania 74605-220, GO, Brazil

\* Correspondence: luizavirginiaduarte@gmail.com

**Abstract:** Precipitation products derived from satellites have emerged as a promising approach for obtaining precipitation estimates, enabling accurate long-term observations and describing the water cycle dynamics from a global scale to a local scale. The quality of these products has improved significantly in the last decades, especially with the emergence of TRMM missions and its successor GPM. The objective of this study was to evaluate the daily, monthly and annual precipitation estimates provided by IMERG version 05 of the GPM, with the data observed by the rainfall stations of the Brazilian Agency of Water and Sanitation (ANA) in the basins of the Brazilian midwest. In order to compare the data, the spatialization of the data of the rainfall stations was performed by means of the ordinary kriging technique, interpolating the data for grids of  $0.1^\circ \times 0.1^\circ$  that correspond to the specialized grids of the GPM satellite. The data were evaluated quantitatively by means of statistical metrics. The GPM satellite precipitation product performed relatively well on a daily scale for regions with smooth topography, and was able to describe the rainfall regime on larger time scales, regardless of the terrain conditions. However, the satellite retrievals were unable to reproduce rainfall extremes in virtually all situations, which may limit their application in frequency analyses.

**Keywords:** IMERG-GPM; precipitation; rain gauges; assessment; statistic



**Citation:** Duarte, L.V.; Formiga, K.T.M.; Costa, V.A.F. Analysis of the IMERG-GPM Precipitation Product Analysis in Brazilian Midwestern Basins Considering Different Time and Spatial Scales. *Water* **2022**, *14*, 2472.

<https://doi.org/10.3390/w14162472>

Academic Editor: Marco Franchini

Received: 27 June 2022

Accepted: 22 July 2022

Published: 10 August 2022

**Publisher's Note:** MDPI stays neutral with regard to jurisdictional claims in published maps and institutional affiliations.



**Copyright:** © 2022 by the authors. Licensee MDPI, Basel, Switzerland. This article is an open access article distributed under the terms and conditions of the Creative Commons Attribution (CC BY) license (<https://creativecommons.org/licenses/by/4.0/>).

## 1. Introduction

Understanding the time–space variability of rainfall is paramount for hydrological applications. In fact, precipitation information at suitable resolutions, both in time and space, is necessary; for instances, for forecasting extreme flooding events; for continuous hydrological simulation that may provide streamflow estimates for the management and operation of hydropower reservoirs and water supply systems; for landslide warnings; and for forcing irrigation models, particularly for agricultural activities in semi-arid environments [1]. In this sense, the definition of strategies for environmental sustainability, flood and drought risk mitigation as well as water resources management is inherently related to the proper stochastic characterization of the precipitation process across a region of interest.

Traditionally, measurements of rainfall amounts are directly obtained from ground-based gauges, and these have constituted the main source of information for hydrological studies. However, rainfall gauging station networks are often unevenly distributed sparsely across space, which imposes difficulties for properly capturing the spatial variability of precipitation systems [2]. In addition, precipitation samples obtained from ground-based gauges are frequently corrupted by long periods of missing data, which may hinder their use for continuous rainfall–runoff modeling and, accordingly, for the indirect estimation of streamflow-related variables [3].

Precipitation information retrieved from satellites has remained a promising approach for characterizing the precipitation process on spatial scales that range from that of the catchment to a near-global scale [4]. Research efforts throughout the last decade have demonstrated potential uses of satellite precipitation products in a variety of applications in hydrology, such as in modeling extreme precipitation events [5,6], rainfall frequency analysis [7], flood frequency analysis [8,9], drought monitoring [10,11] and forecasting [12,13], rainfall–runoff simulation [14–16], and in the planning and management of water resources systems [17]. Previous works have also indicated that resorting to satellite estimates may be advantageous for characterizing the precipitation process in regions where ground-based networks are insufficient, and where other estimation approaches, such as those involving radars, are unable to provide reliable estimates of rainfall amounts [6,18].

The accuracy of precipitation products has considerably increased in the last years [19], particularly since the launching of the Tropical Rainfall Measuring Mission (TRMM) as well as its successor, the Global Precipitation Measurement (GPM). The main purpose of these missions is to provide high-quality and high-resolution global precipitation estimates [20], which could be utilized for real-time monitoring as well as for short-term weather forecasting [21]. GPM, which originated from a joint initiative of the National Aeronautics and Space Administration (NASA) and the Japanese Aerospace Exploration Agency (JAXA), was launched in February 2014. It comprises a large group of international space agencies that includes the Indian Space Research Organization (ISRO), the National Oceanic and Atmospheric Administration (NOAA), and the European Organization for the Exploitation of Meteorological Satellites (EUMETSAT), among others [22,23]. Through improving the estimation of precipitation on a global scale, the GPM mission may enhance knowledge of precipitation systems in addition to the resulting variabilities from other components of the water cycle. Also, short-term weather forecasting and 4-dimensional reanalyses, such as measurements of space–time variabilities in global precipitation, permit us to better understand the following: (i) storm structures, (ii) water/energy balance, (iii) freshwater resources, and (iv) interactions between precipitation and other climate parameters. These fields may all benefit from provided GPM information [24].

In general terms, rainfall amounts are indirectly estimated from satellites by resorting to retrieval algorithms that integrate information from distinct sensors [25]. For the GPM mission, such a combination is performed by integrated multi-satellite retrievals for GPM (IMERG), which merge and interpolate data from a set of passive microwave sensors from the GPM constellation, as well as from information stemming from infrared counterparts; these provide a precipitation product with a spatial resolution of  $0.1^\circ \times 0.1^\circ$ , and a sampling frequency of 30 min across the globe [22].

Although the main objective of the GPM mission is to provide a high-quality precipitation product, it has been widely acknowledged in the literature that the use of retrieval algorithms, no matter how complex, always introduces bias to precipitation estimates [6]. Such bias usually manifests itself distinctly with respect to precipitation amounts, and may furthermore be amplified by climate [26,27] and complex terrain conditions [6]. Moreover, retrieval errors may strongly depend on the aggregation time scales; these errors are usually larger for shorter time scales (e.g., hourly or daily) and considerably smaller for longer ones (e.g., monthly or annual) [19]. These facts have prompted a plethora of studies that assessed the performances of distinct retrieval algorithms in different parts of the world by comparing satellite estimates with ground-based measurements (which are, more often than not, erroneously assumed to be error-free), as well as studies that developed mathematical models for bias correction [6,28–35].

With respect to performance assessment, the IMERG–GPM algorithm has been highlighted for having good overall agreement with ground information, particularly for short time scales, compared to other established precipitation products. In fact, a recent study by Tang et al. (2016) [36] indicated that the IMERG product outperformed its TRMM multi-satellite precipitation analysis (TMPA) 3B42V7 and 3B42RT counterparts, for both daily and sub-daily time scales, in Chinese catchments. These findings were supported by Sharifi,

Steinacker and Saghafian (2016) [37], who compared the IMERG and TRMM products on a daily scale in Iran. Nonetheless, since the performances of retrieval algorithms often vary with climate and topography [6], these conclusions cannot be readily generalized. As a result, suitability assessments for distinct precipitation products should be carried out for each particular study region.

In view of the foregoing, the objective of this study is to evaluate the performance of IMERG-GPM version 05, on daily, monthly and annual scales, for the Brazilian midwestern region. In order to conduct this evaluation, we compare the satellite retrievals with information derived from the rainfall gauging network operated by the Brazilian Agency of Water and Sanitation (Agência Nacional de Águas e Saneamento Básico, ANA), after first performing spatialization to match the satellite resolution for the Meia Ponte and the Bois River catchments. The Brazilian midwestern region is a relatively poorly gauged area [29,35], with a complex climate that is influenced by a variety of atmospheric systems [38]. The area presents marked seasonal features that are known to affect the performance of satellite precipitation products [6]. Previous research on this study region [29,35] has suggested that the TRMM products, which are frequently used as data sources in tropical areas, may present significant biases during the wet season, which in turn provide some justification for performing similar evaluations with the IMERG-GPM counterpart. The remainder of this paper is organized as follows: Section 2 presents the material and methods, with a brief description of the study area and the data, as well as the methods utilized for data quality checking for interpolating the ground-based rainfall amounts and for performance assessment. Section 3 comprises the main results as well as a discussion of them with respect to previous research. Finally, in Section 4, conclusions and research developments are addressed.

## 2. Materials and Methods

### 2.1. Study Area

The study area encompasses the Meia Ponte River catchment, located in the central region of the Brazilian state of Goiás, and the Bois River catchment, located at the southern portion of the state (Figure 1). The Meia Ponte River catchment drains an area of 14,819 km<sup>2</sup>, amounting to approximately 3.6% of the territory of Goiás. It is a densely populated region, with about  $3.131 \times 10^6$  inhabitants concentrated in the municipalities of Goiânia, Aparecida de Goiânia, Anápolis, Senador Canedo and Itumbiara. The catchment is characterized by a tropical savanna climate, with a dry season spanning from April to September and a wet season between October and March. The temperature ranges from 17 °C to 31 °C, whilst the mean annual rainfall varies from 1400 to 1600 mm [39].

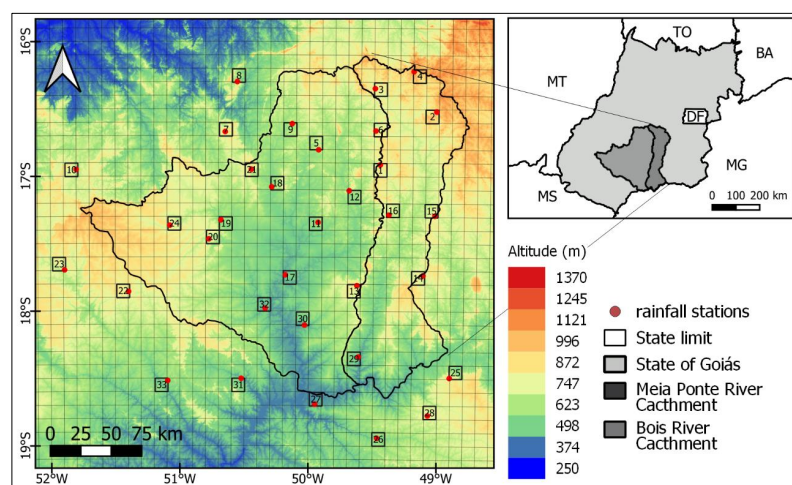


**Figure 1.** Locations of the Meia Ponte and Bois River catchments, rainfall gauging stations, elevations and sampling points utilized in this study. Black squares represent the 33 gauging stations (shown as reference numbers; see Table 1) utilized in the comparison with the  $0.1^\circ \times 0.1^\circ$  GPM pixels.

**Table 1.** Rainfall gauging stations utilized for the estimation of spatialized precipitation and for comparison with the GPM data.

Reference Number in Figure 1	Code	Rainfall Gauging Station	Longitude	Latitude	Elevation (m)	Mean Annual Rainfall (mm)
1	1649001	Aragoiânia	−49.4522	−16.9119	878	1711
2	1649004	Goianópolis	−49.0203	−16.5164	1007	1579
3	1649006	Inhumas	−49.495	−16.3467	746	1215
4	1649009	Ouro Verde de Goiás	−49.1978	−16.2186	1077	1159
5	1649010	Palmeiras de Goiás	−49.9286	−16.8031	605	1183
6	1649012	Trindade	−49.4878	−16.6611	781	1056
7	1650000	Cachoeira de Goiás	−50.6492	−16.6694	763	1140
8	1650001	Córrego do Ouro	−50.5567	−16.2983	565	1494
9	1650003	Turvânia	−50.1328	−16.6094	637	1372
10	1651000	Caiapônia	−51.7994	−16.9497	700	1300
11	1749000	Edéia (Alegrete)	−49.9303	−17.3414	590	1051
12	1749001	Fazenda Boa Vista	−49.6908	−17.1056	550	1147
13	1749002	Joviânia	−49.6264	−17.8094	845	1419
14	1749003	Morrinhos	−49.1153	−17.7328	808	1087
15	1749005	Piracanjuba	−49.0272	−17.2894	779	1543
16	1749009	Cromínia	−49.3828	−17.2847	694	1513
17	1750000	Barra do Monjolo	−50.1808	−17.7322	458	1151
18	1750001	Fazenda Nova do Turvo	−50.2894	−17.0792	529	1265
19	1750004	Ponte Rodagem	−50.6819	−17.3253	551	1123
20	1750008	Fazenda Paraíso	−50.7742	−17.4658	643	1263
21	1750013	Paraúna	−50.4469	−16.9489	684	1564
22	1751001	Ponte Rio Doce	−51.3967	−17.8564	751	1106
23	1751002	Benjamin Barros	−51.8922	−17.695	726	1550
24	1751004	Montividiu	−51.0767	−17.3647	734	1128
25	1848008	Brilhante	−48.9028	−18.4922	795	1356
26	1849000	Ituiutaba	−49.4631	−18.9411	498	1437
27	1849002	Ipiaçú	−49.9486	−18.6919	444	1447
28	1849006	Avantiguara	−49.0697	−18.7719	794	1316
29	1849016	Ponte Meia Ponte	−49.6114	−18.3394	483	1286
30	1850001	Fazenda Aliança	−50.0314	−18.1047	451	1307
31	1850002	Quirinópolis	−50.5219	−18.5011	443	1592
32	1850003	Maurilândia	−50.3372	−17.9797	479	1230
33	1851001	Campo Alegre	−51.0936	−18.5178	569	1845

The Bois River catchment, in turn, amounts to an area of 35,435 km<sup>2</sup>, which corresponds to 9% of the area of Goiás. Forty-three municipalities, which comprise 651,391 inhabitants, are partially or entirely contained in this catchment. According to Santos, Bayer and Carvalho (2008) [40], this is also a region with marked seasonality, having a dry period between May and September and a wet counterpart from October to April. Mean annual rainfall amounts range from 1400 mm to 1800 mm.

## 2.2. Data from Ground-Based Rainfall Gauging Stations

Daily rainfall amounts were obtained from the digital platform of the Brazilian Agency of Water and Sanitation (Agência Nacional de Águas e Saneamento Básico, ANA). A collection of 37 gauging stations with a period of record spanning from 1988 to 2017 were initially selected for this study. In order to fill missing data that amounted to 31 days for the 1750000 gauging station, 13 days for the 1750001 and a single day for the 1750008 gauging station, we resorted to using simple linear regression. The procedure, which was performed with the “hyfo” R package [41], is as follows: for a given gauging station with data to be filled, the candidate neighboring gauges are ranked based on their correlation coefficients; next, simple linear regression equations are derived by using the data from each candidate as explanatory variables; finally, for each day with missing data the rainfall amount estimate is derived from the most correlated candidate with available data. We acknowledge that this simple linear regression may not be the most accurate alternative to fill missing precipitation data on a daily scale [42], and that the predictive abilities of the obtained regression models are relatively low ( $R^2 < 0.30$ ). However, since the number of missing data is small, we believe that the use of this simplified tool did not strongly affect the performance assessment.

Additional data quality checks comprised excluding gauging stations with more than 20% of missing data in addition to those that received annual rainfall amounts larger than 2500 mm or smaller than 1000 mm, which are deemed unreasonable values for the study region on the basis of the 30-year average annual precipitation.

After the data quality check and the filling of missing data, four gauging stations which presented anomalous behaviors with respect to the mean annual rainfall (values less than 1000 mm) were discarded. The gauges that were retained for analyses are shown in Table 1. Finally, for assessing the performance of the GPM precipitation product, whose data are available from 2014 onwards, the daily rainfall amounts recorded in the water year of September 2016–August 2017 were utilized. We note that this decision resulted from the large amount of missing data prior to 2016 and from 2017 onwards in most of the rainfall gauging stations utilized in our study; this could introduce high levels of bias in the comparison. On the other hand, 2017 presented an annual rainfall amount relatively close to the long-term average (1339 mm and 1500 mm, respectively, for the Meia Ponte River catchment), which may, at least to some extent, attenuate the effects of low data availability in subsequent analyses.

### *2.3. Data from the GPM Precipitation Product*

Satellite precipitation estimates were retrieved with IMERG, the algorithm developed by the GPM team to provide the precipitation product. The algorithm's fifth version (level 03), which provides rainfall estimates with a spatial resolution of  $0.1^\circ \times 0.1^\circ$  and a 30-min sampling frequency, was utilized. The algorithm was designed to combine information from multiple international satellites and develop long-term precipitation records in uniformly distributed pixels across the globe [43].

For our analyses, the IMERG-GPM product, provided in format HDF5 by NASA, was initially imported to the software ArcGIS (version 10.6, Esri, RedLands, CA, USA). Next, precipitation estimates were extracted for the water year of 2017 and for those pixels located between  $52^\circ$  and  $19^\circ$  S and  $19^\circ$  and  $16^\circ$  W, which entirely enclosed the study area. The satellite retrievals were then aggregated for daily, monthly, and annual time scales and compared to spatialized and raw ground-based rainfall measurements.

### *2.4. Data Interpolation*

Data derived from rainfall gauges were interpolated in order to form uniform grids with the same spatial resolution as the GPM satellite retrievals (i.e.,  $0.1^\circ \times 0.1^\circ$  or approximately 11 km). The interpolation was performed in ArcGIS (version 10.6) by using the ordinary kriging technique, a method that assumes a spatial Gaussian field with a covariance function defined by a semivariogram [44]. Ordinary kriging is a widespread interpolation technique that frequently outperforms alternative methods when dealing with precipitation data [45]. For fitting the theoretical Gaussian field to the empirical sample points, a spherical semivariogram was utilized with a range of 150 km and a cutoff point of 300 km. Then, the rainfall amounts were estimated at the vertices of each pixel defined by the IMERG-GPM product and averaged over these points in order to match the satellite's resolution.

Once the precipitation time series were interpolated, spatialized average values were computed for both the catchments' drainage areas and for each of the gridded elements with ground-based gauges; this allows the identification of those regions across the study area in which the satellite retrievals present larger deviations with respect to the measured rainfall amounts. The comparisons comprised the period of record spanning from 1 September 2016 to 31 August 2017.

### *2.5. Comparison of Precipitation Amounts*

The performance assessment of the IMERG-GPM algorithm was based on the computation of the goodness-of-fit metrics presented in Table 2 [46], which are intended to provide a comprehensive evaluation of the satellite product. Absolute metrics such as the mean absolute error (MAE) and the root mean square error (RMSE) assess the overall agreement between ground-based and satellite estimates, whereas the mean error (ME) and the percent bias (PBIAS) disclose the existence of systematic errors which result in under- or overestimation. Finally, we also utilized as benchmarks the Nash–Sutcliffe efficiency crite-

tion (NSE) as well as the coefficient of persistence (CP); the former is a common metric that is used in hydrological applications but sometimes criticized by misinterpretations [47]; the latter, which uses the previous day’s observed precipitation as an alternative to the satellite information, provides a naïve yet usually more robust benchmark. Some of these indexes, such as the MAE and RMSE, provide similar information regarding model performance; however, marked distinctions among them might indicate a more general lack of fit or large deviations solely with respect to higher-order statistics [48].

**Table 2.** Goodness-of-fit metrics utilized in the comparison of the GPM precipitation product and the ground-based measurements.

Goodness-of-Fit Metrics	Description	Equation	Perfect Value
Coefficient of correlation (CC)	Evaluates the agreement between satellite retrievals and ground-based rainfall measurements	$CC = \frac{\sum_{i=1}^n (O_i - \bar{O})(E_i - \bar{E})}{\sqrt{\sum_{i=1}^n (O_i - \bar{O})^2} \cdot \sqrt{\sum_{i=1}^n (E_i - \bar{E})^2}}$	1
Mean absolute error–(MAE) mm	Measures the mean value of the absolute errors	$MAE = \frac{1}{n} \sum_{i=1}^n  E_i - O_i $	0
Root mean square error (RMSE) mm	Measures the mean value of the squared errors	$RMSE = \sqrt{\frac{1}{n} \sum_{i=1}^n (E_i - O_i)^2}$	0
Percent bias (PBIAS) %	Expresses systematic errors	$PBIAS = \frac{\sum_{i=1}^n (E_i - O_i)}{\sum_{i=1}^n O_i} \times 100$	0
Mean Error (ME) mm	Expresses the uncertainty in a measurement	$ME = \frac{1}{n} \sum_{i=1}^n (E_i - O_i)$	0
Nash–Sutcliffe Efficiency (NSE)	Evaluates the predictive ability of hydrological models.	$NSE = 1 - \frac{\sum_{i=1}^n (E_i - O_i)^2}{\sum_{i=1}^n (O_i - \bar{O})^2}$	1
Coefficient of Persistence (CP)	Compares the performance of the model being used and performance of the persistent	$CP = 1 - \frac{\sum_{i=2}^n (E_i - O_i)^2}{\sum_{i=1}^{n-1} (O_{i+1} - O_i)^2}$	1

Note(s): **n** is the number of sample points, **O** denotes the ground-based rainfall measurements, and **E** corresponds to the IMERG-GPM retrievals.

In addition to the interpolated rainfall, we also evaluated the performances of the retrieval algorithm with the raw data extracted from the gauges as a means of assessing potential benefits or shortcomings of the kriging procedure. Furthermore, we computed the metrics for those ground-based rainfall amounts that equaled or exceeded the 95th-quantile data from each gauging station (from the raw data set) in order to assess the goodness-of-fit of the IMERG-GPM product regarding daily rainfall extremes.

### 3. Results

#### 3.1. Daily Time Scale

A comparison of satellite retrievals and rainfall gauging measurements averaged over the catchments’ drainage areas is presented in Figure 2 for the Meia Ponte River catchment, and in Figure 3 for the Bois River catchment. It is possible to note that, for the former, the temporal coherence of rainfall events is reasonably reproduced by the satellite product, as demonstrated by the relatively high CC, albeit with a tendency to overestimate; this is detected from the values of the ME and PBIAS. The value of the RMSE, in turn, is almost twice that of the MAE, which suggests that the higher-order statistics are not properly reproduced by the satellite retrievals—this may constitute a major limitation for utilizing the IMERG-GPM product for both block-maxima and peaks-over-threshold frequency analysis. Finally, the benchmarks NSE and CP indicate that the satellite product has larger predictive skills than the observed mean and the observed previous day’s precipitation data, respectively, even though their values are relatively close to zero.

For the Bois River catchment, the overall tendency of overestimation is even more pronounced, with higher values for the ME and PBIAS, as compared to the Meia Ponte data set. Moreover, a poorer representation of the temporal dynamics of the observed rainfall is perceived, with some lag between GPM retrievals and observed events throughout most of the period of record. Finally, the distinctions among the RMSE and MAE values are also noticeable, suggesting an unsuitable description of rainfall extremes by the satellite retrieval; additionally, both benchmarks are negative, indicating that the mean and/or the previous day’s observed precipitation are preferable for prediction. On the other hand, the dry season was reasonably described in both catchments, which suggests at least for the

study area that the GPM product is sufficiently accurate for detecting non-rainfall events. We note, however, that this is a poorly gauged catchment, in which many of the rainfall gauging stations are located in areas with more complex terrain and stronger topographic gradients (Figure 1). At least to some extent, this fact may explain the poorer performance of the IMERG-GPM product in the Bois River catchment. In effect, it is well established that most satellite products are unable to properly reproduce rainfall regimes in regions with complex topographies [6].

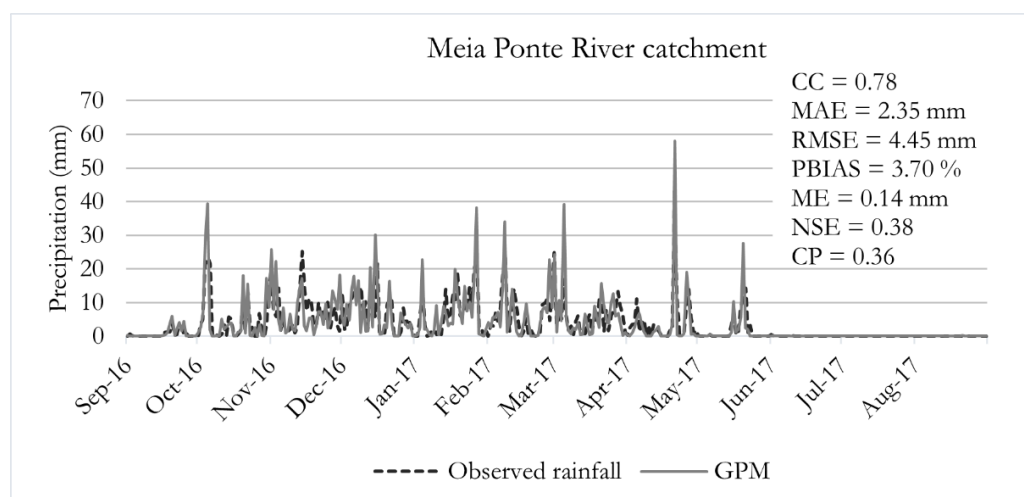


**Figure 2.** Comparison of the daily precipitation, as obtained from the GPM and the ground rainfall gauging network, averaged over the area of the Meia Ponte River catchment.

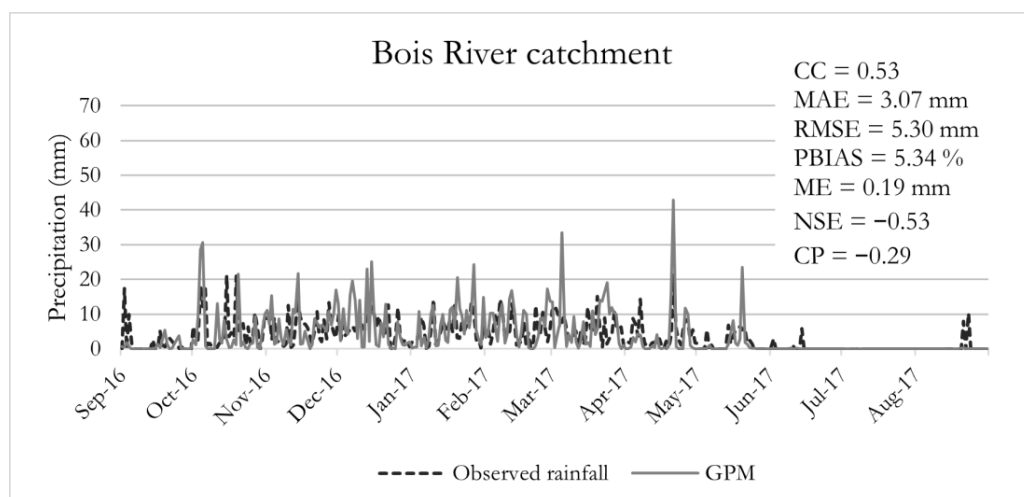


**Figure 3.** Comparison of the daily precipitation, as obtained from the GPM and the ground rainfall gauging network, averaged over the area of the Bois River catchment.

Figure 4 depicts scatterplots for the GPM precipitation estimates and the observed rainfall amounts. For the Meia Ponte River catchment (left panel), a linear functional form may be visualized, despite the large dispersion of the errors for precipitation amounts larger than 10 mm, which entailed a value of 0.61 for the coefficient of determination  $R^2$ , and some degree of deviation from the 1:1 line. For the Bois River catchment (right panel), on the other hand, the linear association is much weaker with  $R^2 = 0.29$ , which indicates that the satellite retrievals are unable to explain the variation in the observed rainfall in this area.

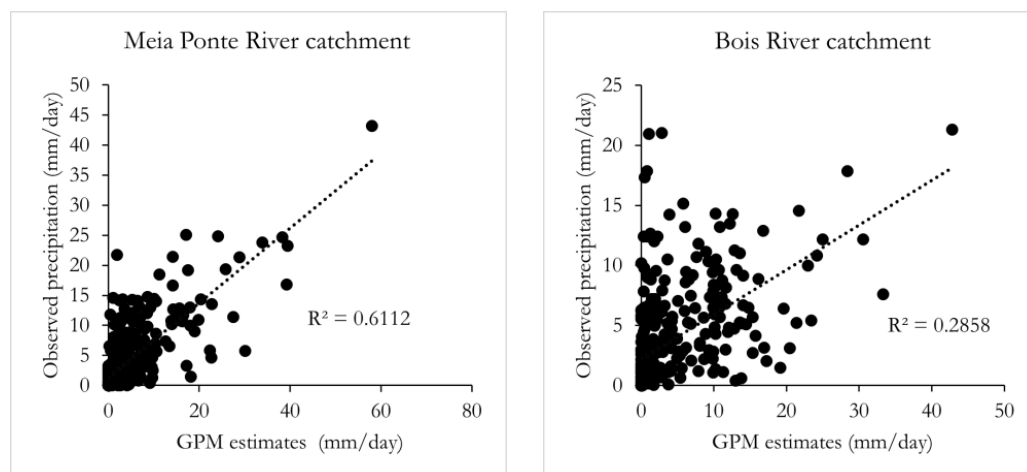


**Figure 4.** Scatterplots of the GPM estimates and the observed precipitation amounts for the Meia Ponte River catchment (left panel) and the Bois River catchment (right panel).

We also compared the daily precipitation of each rainfall gauging station, after interpolation and with raw data, with those obtained from the corresponding grid of the GPM product. Results are summarized in Table 3 for the Meia Ponte River catchment, and in Table 4 for the Bois River catchment. One may notice that for the former, the metrics across gauges for the interpolated rainfall are somewhat similar, with exception of the PBIAS, which presented mostly positive low values, but indicated a tendency to underestimate (slightly) in the Meia Ponte gauging station. Hence, the performance of the GPM product did not present marked spatial variability in this catchment. We also note that despite entailing similar values for most metrics, using the raw data affected the systematic biases either by changing their signs or by increasing their values (in absolute terms). This fact would favor the interpolation approach. On the other hand, the benchmarks suggest that satellite retrievals are closer to the raw data, whose use entailed substantial improvements in the values of both the NSE and CP—for the interpolated rainfall, these are mostly negative or close to zero.

**Table 3.** Goodness-of-fit metrics for interpolated and raw (in parentheses) daily precipitation data from four gauging stations located in the Meia Ponte River catchment.

Gauging Station with Reference Number	CC	MAE (mm)	RMSE (mm)	PBIAS (%)	ME (mm)	NSE	CP
16-Cromínia	0.59 (0.57)	3.31 (4.07)	7.29 (9.48)	3.10 (−9.4)	0.11 (−0.39)	−0.16 (0.27)	0.02 (0.56)
2-Goianápolis	0.63 (0.48)	3.40 (4.17)	6.78 (8.94)	4.57 (3.7)	0.17 (0.14)	0.07 (0.04)	0.37 (0.43)
3-Inhumas	0.53 (0.49)	3.47 (3.97)	7.21 (8.66)	6.01 (15.6)	0.22 (0.52)	−0.20 (0.08)	0.17 (0.47)
29-Meia Ponte	0.57 (0.51)	3.37 (3.84)	7.79 (9.11)	−1.03 (2.7)	−0.04 (0.09)	0.05 (0.17)	0.33 (0.47)

Inspection of Table 4, in turn, indicates a much larger variation in the values of the goodness-of-fit metrics, and an overall worse performance with respect to the interpolated rainfall in the Bois River catchment. In effect, whilst most values of the CCs ranged from 0.39 to 0.50, suggesting a poorer description of the temporal dynamics of the observed rainfall, the values of RMSE surpass, in many cases, more than 20% of those in the Meia Ponte catchment. High levels of variation are also verified for the PBIAS, and the tendency of overestimation is much stronger in the Bois River catchment—in some cases, systematic

errors larger than 15% were verified. Of course, this may have stemmed from the inaccurate spatialization of the observed rainfalls in some portions of the catchment, as well as from the locations of the rainfall gauging stations in areas with complex terrain. However, our results suggest that the GPM product was unable to retrieve the real evolution of the daily precipitation activities across this entire region, and this certainly calls for further investigation in regard to potential causes of this phenomenon.

**Table 4.** Goodness-of-fit metrics for interpolated and raw (in parentheses) daily precipitation data from 12 gauging stations located in the Bois River catchment.

Gauging Station with Reference Number	CC	MAE (mm)	RMSE (mm)	PBIAS (%)	ME (mm)	NSE	CP
17-Barra do Monjolo	0.61 (0.44)	3.15 (3.93)	6.99 (9.26)	22.05 (23.6)	0.7 (0.74)	−0.36 (−0.11)	−0.16 (0.31)
11-Edeia (Alegrete)	0.40 (0.35)	4.04 (4.58)	9.82 (11.09)	1.32 (30.4)	0.05 (0.88)	−0.33 (−0.24)	0.12 (0.37)
30-Fazenda Aliança	0.49 (0.38)	3.45 (4.36)	7.55 (10.58)	2.28 (−1)	0.08 (−0.04)	−0.25 (0.01)	0.05 (0.39)
12-Fazenda Boa Vista	0.65 (0.6)	3.22 (3.86)	6.42 (7.92)	−0.24 (15.8)	−0.01 (0.5)	0.17 (0.29)	0.4 (0.59)
18-Fazenda Nova do Turvo	0.44 (0.39)	3.61 (4.16)	8.86 (10.88)	7.95 (5.5)	0.27 (0.19)	−0.89 (−0.16)	−0.35 (0.32)
20-Fazenda Paraíso	0.39 (0.28)	3.81 (4.63)	8.54 (10.31)	3.37 (5.9)	0.12 (0.2)	−0.26 (−0.25)	0.22 (0.34)
13-Joviânia	0.70 (0.61)	3.04 (3.87)	6.36 (8.47)	11.24 (−0.2)	0.39 (−0.01)	0.19 (0.31)	0.34 (0.57)
32-Muarilândia	0.46 (0.37)	3.44 (4.06)	7.84 (9.56)	9.68 (8.3)	0.32 (0.28)	−0.41 (−0.18)	−0.03 (0.38)
24-Montividiu	0.50 (0.47)	3.34 (3.86)	7.37 (8.4)	25.18 (25.9)	0.78 (0.8)	−0.27 (−0.04)	0.07 (0.37)
5-Palmeiras de Goiás	0.58 (0.46)	3.37 (4.06)	6.71 (8.78)	14.25 (14.5)	0.46 (0.47)	−0.25 (0)	0.13 (0.47)
21-Paraúna	0.41 (0.4)	4.08 (4.86)	10.56 (12.1)	1.32 (−7.7)	0.05 (−0.33)	−0.48 (−0.11)	0.05 (0.4)
19-Ponte Rodagem	0.41 (0.28)	3.87 (4.81)	8.92 (11.36)	11.31 (24.8)	0.39 (0.76)	−0.52 (−0.3)	0.06 (0.34)

As for the comparison between raw and interpolated data, similar remarks to those in the Meia Ponte River catchment can be made: the PBIAS is strongly affected by the sampling approach, and the use of raw data increased the values of the benchmarks. However, compared to the Meia Ponte river catchment, such increases in the NSE and CP were less noticeable. Overall, the interpolation procedure did not seem to be beneficial, which could be at least to some extent anticipated, based on the large distances between the rainfall gauging stations. The incorporation of covariates such as topographic features to the kriging procedure may improve the interpolation results, and this will be addressed in future research.

Finally, the goodness-of-fit assessment regarding observed daily extreme events, as materialized by the empirical 95th-quantile data from each rainfall gauging station, are shown in Tables 5 and 6 for the Meia Ponte and the Bois River catchments, respectively. It is generally possible to note that the values of metrics such as RMSE and MAE are close to the empirical quantiles themselves, which indicates a strong disagreement between satellite retrievals and ground-based information for large rainfall amounts. Moreover, the benchmarks are mostly negative, and the values of CCs are low, which may be due to

poorer performance of the retrieval algorithm for extreme rainfall conditions, or because such extreme events are not being recorded on the same days by the satellite and the gauges. Overall, as previously hypothesized, the IMERG-GPM product was unable to reproduce daily rainfall extremes, which might limit its use for frequency analysis and risk assessment.

**Table 5.** Goodness-of-fit metrics for daily rainfall amounts above the 95th empirical quantiles from four gauging stations located in the Meia Ponte River catchment.

Gauging Station with Reference Number	95th Empirical Quantile Rainfall Gauging Station	95th Empirical Quantile GPM	CC	MAE	RMSE	PBIAS	ME	NSE	CP
16-Cromínia	25.84	19.26	0.62	25.83	28.99	−57.6	−24.8	−2.56	−0.44
2-Goianápolis	23.92	24.12	0.33	19.02	23.39	−50.4	−17.91	−3.48	−1.65
3-Inhumas	21.42	21.39	0.55	22.1	24.59	−54.1	−20.73	−3.78	−2.34
29-Meia Ponte	25.26	21.21	0.43	21.74	26.05	−58.7	−20.76	−2.14	−0.34

**Table 6.** Goodness-of-fit metrics for daily rainfall amounts above the 95th empirical quantiles from 12 gauging stations located in the Bois River catchment.

Gauging Station with Reference Number	95th Empirical Quantile Rainfall Gauging Station	95th Empirical Quantile GPM	CC	MAE	RMSE	PBIAS	ME	NSE	CP
17-Barra do Monjolo	22.30	21.66	−0.18	20.62	26.44	−51.6	−17.39	−4.8	−4.14
11-Edeia (Alegrete)	21.60	20.57	0.41	27.02	31.15	−62.5	−25.32	−3.35	−0.7
30-Fazenda Aliança	27.18	21.34	0.21	28.15	32.11	−68	−26.69	−4.52	−1.55
12-Fazenda Boa Vista	20.74	18.06	0.82	19.13	20.65	−48.5	−17.56	−0.87	−0.78
18-Fazenda Nova do Turvo	22.72	19.64	0.52	34.62	38.2	−69	−33.9	−4.4	−0.61
20-Fazenda Paraíso	24.70	19.64	0.06	25.29	29.07	−74.7	−25.29	−5.79	−2.62
13-Joviânia	24.82	24.29	0.41	22.34	24.61	−42.4	−16.54	−1.68	−0.07
32-Muarilândia	22.90	18.37	−0.28	21.1	25.73	−52.1	−15.6	−4.64	−1.16
24-Montividiu	19.36	20.04	0.33	19.13	22.35	−54.2	−19.13	−4.73	−1.73
5-Palmeiras de Goiás	18.50	19.83	0.57	23.57	26.8	−59.8	−21.43	−2.25	−0.36
21-Paraúna	28.18	16.54	−0.2	35.45	41.01	−47	−19.81	−3.75	−1.42
19-Ponte Rodagem	22.74	20.87	−0.13	28.19	35.59	−62.2	−22.89	−3.44	−1.22

### 3.2. Monthly Time Scale

Figure 5 depicts the comparison of the monthly precipitation for the rainfall gauging stations located in the Meia Ponte River catchment; the values of the goodness-of-fit metrics are presented in Table 7. A similar plot is shown in Figure 6 for the Bois River catchment, with the metrics being provided in Table 8. One may observe that, as expected for larger time scales which smooth out strong variations in precipitation activity on a daily or sub-daily scale, the performance of the IMERG-GPM product considerably improves. In effect, the values of CCs were larger than 0.90 in all situations, although the tendency to overestimate still persisted in some gauging stations, such as Montividiu (PBIAS = 25.18%). In all cases, the values of the NSE and CP indicate that the satellite product has considerably greater predictive skills as compared to the benchmarks. Again, we note that a higher level of variability in the goodness-of-fit metrics was verified for the Bois River catchment, and the values of the RMSE and MAE present marked distinctions for this area, which may suggest that the GPM product could not properly capture the spatial patterns of variability and describe the rainfall behavior during the wet season, even on a monthly time scale, for this region.

On the other hand, when precipitation amounts are averaged over the entire areas of the catchments, the performance of the GPM product is suitable and similar for both geographical regions. In fact, as depicted in Figure 7, the satellite retrievals present good agreement with spatialized gauge data for all months, and are able to explain 98% (left panel) and 99% (right panel) of the latter's variability for the Meia Ponte and the Bois River catchments, respectively. In other words, the averaging procedure across large

extensions smoothed out the larger variations in particular locations of the catchment that were verified in the previous analyses, hence improving GPM performance overall.

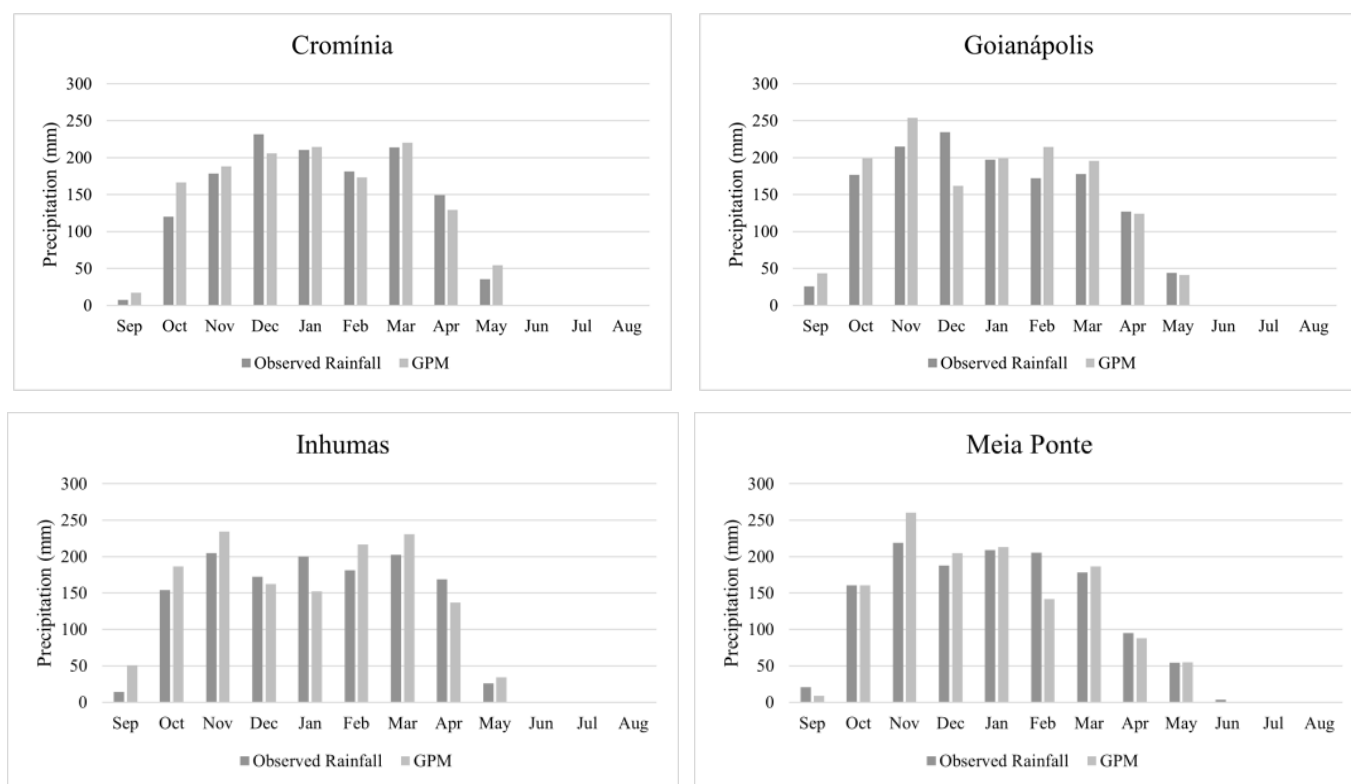
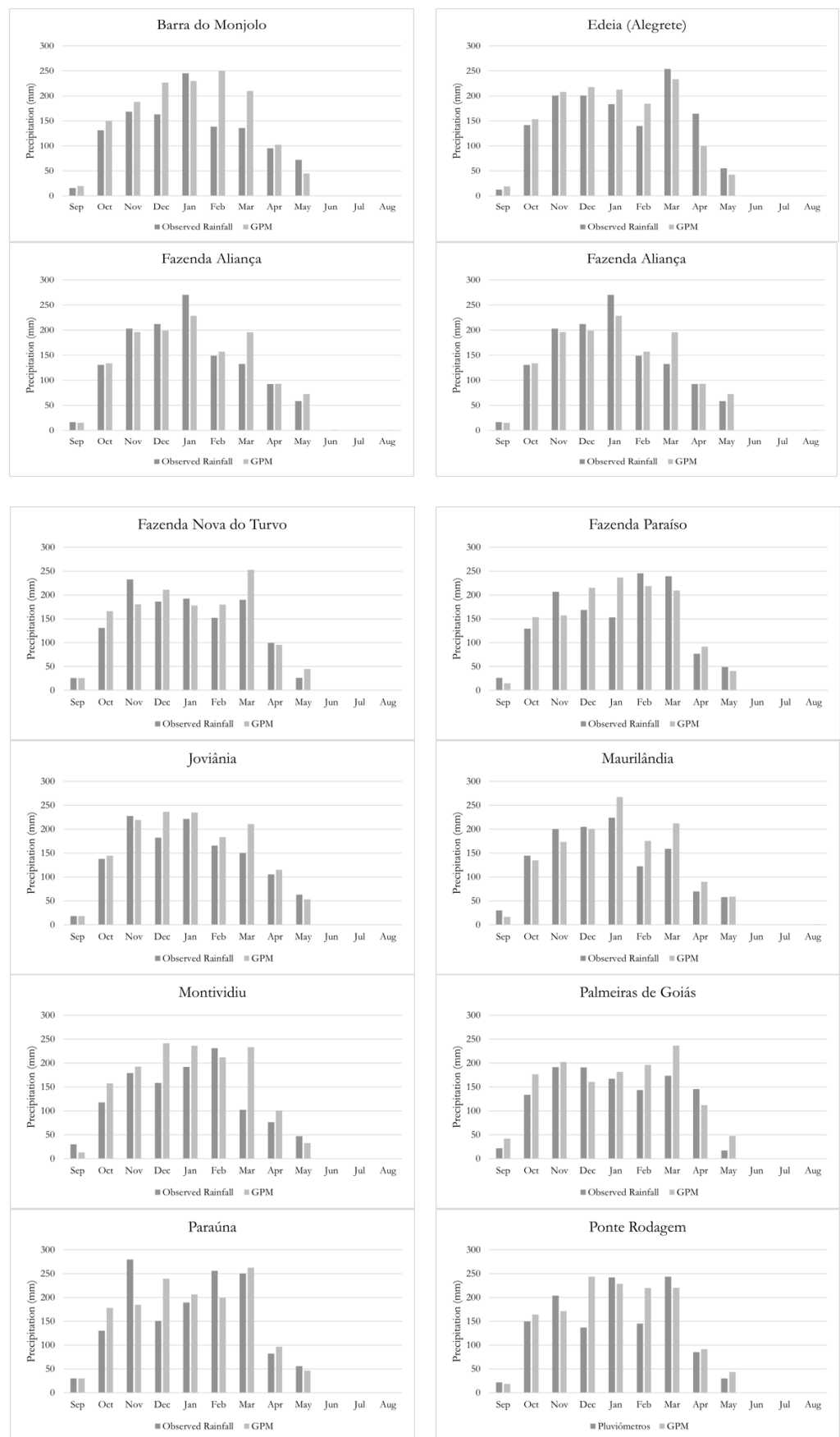


**Figure 5.** Monthly rainfall amounts as obtained from the GPM product and ground-based gauges for the Meia Ponte River catchment.

**Table 7.** Goodness-of-fit metrics for monthly precipitation data from four gauging stations located in the Meia Ponte River catchment.

Gauging Station with Reference Number	CC	MAE (mm)	RMSE (mm)	PBIAS (%)	ME (mm)	NSE	CP
16-Crominia	0.98	12.41	17.96	0.03	3.43	0.96	0.9
2-Goianópolis	0.95	18.26	28.45	0.05	5.22	0.9	0.75
3-Inhumas	0.96	21.68	27.06	0.06	6.64	0.91	0.84
29-Meia Ponte	0.97	13.23	23.11	−1.03	−1.14	0.93	0.83

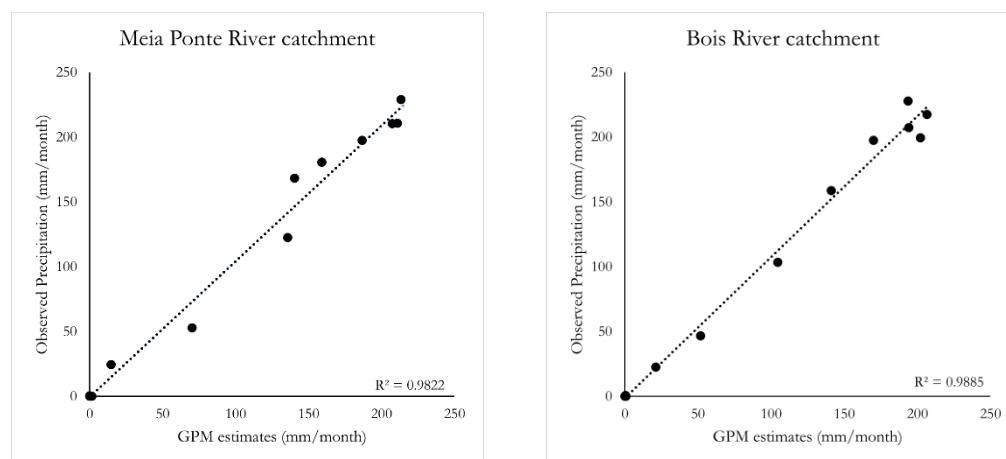
As for the other goodness-of-fit metrics, the GPM product presented values of 10.9 mm for the MAE, 13.51 mm for the RMSE, 4.31% for the PBIAS, 4.81 mm for the ME, 0.97 for the NSE and 0.94 for the CP in the Meia Ponte River catchment; and 9.55 mm for the MAE, 14.64 for the RMSE, 7.46% for the PBIAS, 7.5 mm for the ME, 0.97 for the NSE and 0.92 for the CP in the Bois River catchment, when compared to gauging measurements. These results indicate a considerable enhancement with respect to the pixel-based analyses, which are again indicative of the potential advantages of averaging the precipitation amounts over larger geographical areas.



**Figure 6.** Monthly rainfall amounts as obtained from the GPM product and ground-based gauges for the Bois River catchment.

**Table 8.** Goodness-of-fit metrics for monthly precipitation data from 12 gauging stations located in the Bois River catchment.

Gauging Station with Reference Number	CC	MAE (mm)	RMSE (mm)	PBIAS (%)	ME (mm)	NSE	CP
17-Barra do Monjolo	0.92	28.63	44.60	0.22	21.41	0.67	0.41
11-Edeia (Alegrete)	0.96	17.89	25.96	0.01	1.49	0.92	0.86
30-Fazenda Aliança	0.97	12.89	22.84	0.02	2.40	0.93	0.85
12-Fazenda Boa Vista	0.97	16.06	22.48	0.00	−0.27	0.93	0.88
18-Fazenda Nova do Turvo	0.95	20.06	28.67	0.08	8.19	0.89	0.76
20-Fazenda Paraíso	0.93	24.58	34.39	0.03	3.64	0.86	0.75
13-Joviânia	0.98	15.12	24.86	0.11	11.93	0.91	0.80
32-Muarilândia	0.96	18.75	27.25	0.10	9.79	0.89	0.78
24-Montividiu	0.91	32.17	49.35	0.25	23.80	0.60	0.17
5-Palmeiras de Goiás	0.94	24.92	31.95	0.14	14.08	0.84	0.67
21-Paraúna	0.96	18.75	27.25	0.10	9.79	0.89	0.78
19-Ponte Rodagem	0.91	32.17	49.35	0.25	23.80	0.60	0.17

**Figure 7.** Scatterplots of monthly rainfall amounts for the GPM retrievals and ground-based gauges in the Meia Ponte (**left** panel) and the Bois River catchments (**right** panel).

### 3.3. Annual Time Scale

The spatial distribution of the annual rainfall amounts for the water year of 2017 is depicted in Figure 8; the spatialized ground-based measurements are shown in the left panel and those of the GPM product are in the middle counterpart. It is possible to observe that as with the other time scales, the GPM product overestimated the precipitation amounts for both catchments; for the maximum values of annual rainfall, the ground-based gauges accumulated 1400 mm while the satellite retrievals obtained 1600 mm. In addition, the satellite product was not able to reproduce the spatial pattern of variability in the observed rainfall. Whereas some variability is verified for the ground-based rainfall data, particularly for the northeastern portion of the Bois River catchment which presents a more complex topography, the satellite estimates are relatively homogeneously distributed across the entire study region. Such a condition resulted in a noticeable gradient in the errors in the southeastern–northwestern direction (right panel of Figure 8). We again hypothesize that the spatial interpolation may play a large role on the rougher behavior verified in the left panel of Figure 8. However, our results suggest that bias correction would be troubling

for annual rainfall amounts in the study area since the regional distinctions in rainfall distribution might not be readily explained by the usual covariates, such as altitude.

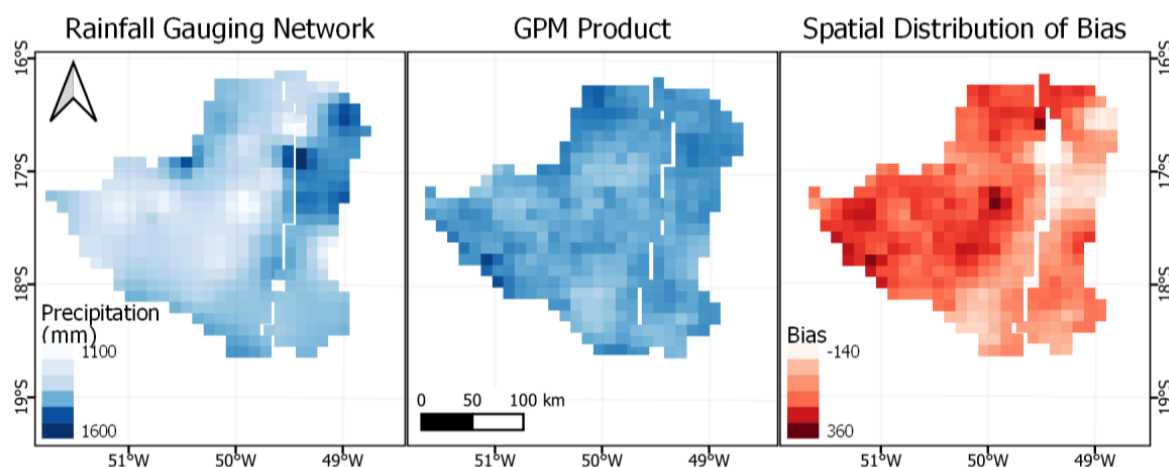


**Figure 8.** Annual rainfall amounts for the water year of 2017, as obtained from the ground-based rainfall gauging network (**left** panel), from the GPM product (**middle** panel) and the spatial distribution of bias (**right** panel).

As a final remark, we note that previous research demonstrated that the GPM product has suitable abilities in describing spatial precipitation patterns, but the rainfall intensities and spatial variability, which are closely linked to seasonality, have some influence on the capability of the GPM retrievals to capture local precipitation patterns [48]. Our results are at least to some extent in agreement with these conclusions. In fact, in many situations, the spatial distribution of rainfall was not properly described by the IMERG satellite retrievals, with a tendency of generating smoother surfaces as compared to the data captured by ground-based information. Nonetheless, as may be inferred from Melo et al., 2015, and Moraes and Gonçalves, 2021 [29,35], the IMERG-GPM may be a preferable alternative for our study region after spatial averaging, as it more properly described the rainfall amounts on a daily time scale. Hence, despite the inaccurate descriptions of daily rainfall extremes, which are not considerably improved under bias correction [6], the short size of our sample, and the relatively poor representation of spatial patterns, we still believe that the IMERG-GPM product may be a useful data source for the Brazilian midwestern region, as compared to well-established alternatives such as TRMM, mainly for continuous rainfall–runoff simulation based on a daily time step, and drought management, which requires data at monthly or longer time scales.

#### 4. Conclusions

The GPM mission has provided a new generation of high-resolution precipitation products that could be utilized in several fields, such as hydrology and climatology. In this paper, the performance of the fifth version of the IMERG retrieval algorithm for the GPM constellation was assessed by comparing its satellite retrievals with ground-based information, on daily, monthly and annual scales throughout the period spanning from September 2016 to August 2017. The study evaluated the precipitation fields and the rainfall amounts, averaged at the catchment scale, for the Meia Ponte and the Bois River catchments, both located in the state of Goiás in the Brazilian midwestern region.

Our results indicated that for the Meia Ponte River catchment, a reasonable agreement between satellite retrievals and ground-based measurements in the precipitation fields was obtained, with a tendency of overestimation in all time scales, by the satellite precipitation products. For the Bois River catchment, which is located in a region with more complex terrain and is less densely gauged, the performance of the satellite product was considerably worse, with a disruption in temporal coherence for daily data, and a

stronger positive systematic bias, as compared to its performance with the Meia Ponte River catchment. When averaged over the catchment area, the precipitation estimates were reasonable for monthly and annual scales, indicating that the averaging procedure smoothed out the largest deviations in some areas of the catchments. Nonetheless, the spatial rainfall patterns were more often than not misrepresented by the IMERG retrievals, which generated oversmoothed surfaces and did not capture local features of the observed rainfall fields. Furthermore, in both spatial scales the most extreme events on a daily scale were not properly reproduced by the satellite product.

Satellite precipitation products are advantageous for practical applications, since they capture in a more effective manner the space–time patterns of precipitation events and are not affected by missing data. Nonetheless, as shown in this study and in several others, due to the indirect mechanisms for estimating rainfall amounts, satellite products are biased—mainly for the most extreme events, which are paramount for design and risk assessment. Hence, despite the technological development applied to the GPM mission for providing high-quality precipitation products, some research effort is still necessary to develop more effective techniques for bias correction. This is envisaged as our next research objective.

**Author Contributions:** L.V.D. wrote the paper and analyzed the data and the results; V.A.F.C. and K.T.M.F. revised the manuscript and analyzed the results. All authors have read and agreed to the published version of the manuscript.

**Funding:** This study was financed by Financiadora de Estudos e Projetos (Finep).

**Acknowledgments:** The authors acknowledge the anonymous reviewers and the editors for their valuable comments and suggestions, which greatly helped improve the paper.

**Conflicts of Interest:** The authors declare no conflict of interest.

## References

1. McMillan, H.; Jackson, B.; Clark, M.; Kavetski, D.; Woods, R. Rainfall Uncertainty in Hydrological Modelling: An Evaluation of Multiplicative Error Models. *J. Hydrol.* **2011**, *400*, 83–94. [[CrossRef](#)]
2. Ning, S.; Wang, J.; Jin, J.; Ishidaira, H. Assessment of the Latest GPM-Era High-Resolution Satellite Precipitation Products by Comparison with Observation Gauge Data over the Chinese Mainland. *Water* **2016**, *8*, 481. [[CrossRef](#)]
3. Anagnostou, E.N.; Maggioni, V.; Nikolopoulos, E.I.; Meskele, T.; Hossain, F.; Papadopoulos, A. Benchmarking High-Resolution Global Satellite Rainfall Products to Radar and Rain-Gauge Rainfall Estimates. *IEEE Trans. Geosci. Remote Sens.* **2010**, *48*, 1667–1683. [[CrossRef](#)]
4. Xu, S.; Shen, Y.; Du, Z. Tracing the Source of the Errors in Hourly IMERG Using a Decomposition Evaluation Scheme. *Atmosphere* **2016**, *7*, 161. [[CrossRef](#)]
5. Xiao, S.; Xia, J.; Zou, L. Evaluation of Multi-Satellite Precipitation Products and Their Ability in Capturing the Characteristics of Extreme Climate Events over the Yangtze River Basin, China. *Water* **2020**, *12*, 1179. [[CrossRef](#)]
6. Ma, Y.; Sun, X.; Chen, H.; Hong, Y.; Zhang, Y. A Two-Stage Blending Approach for Merging Multiple Satellite Precipitation Estimates and Rain Gauge Observations: An Experiment in the Northeastern Tibetan Plateau. *Hydrol. Earth Syst. Sci.* **2021**, *25*, 359–374. [[CrossRef](#)]
7. Gado, T.A.; Hsu, K.; Sorooshian, S. Rainfall Frequency Analysis for Ungauged Sites Using Satellite Precipitation Products. *J. Hydrol.* **2017**, *554*, 646–655. [[CrossRef](#)]
8. Dis, M.O.; Anagnostou, E.; Mei, Y. Using High-Resolution Satellite Precipitation for Flood Frequency Analysis: Case Study over the Connecticut River Basin. *J. Flood Risk Manag.* **2018**, *11*, S514–S526. [[CrossRef](#)]
9. Gao, Z.; Long, D.; Tang, G.; Zeng, C.; Huang, J.; Hong, Y. Assessing the Potential of Satellite-Based Precipitation Estimates for Flood Frequency Analysis in Ungauged or Poorly Gauged Tributaries of China’s Yangtze River Basin. *J. Hydrol.* **2017**, *550*, 478–496. [[CrossRef](#)]
10. Zambrano, F.; Wardlow, B.; Tadesse, T.; Lillo-Saavedra, M.; Lagos, O. Evaluating Satellite-Derived Long-Term Historical Precipitation Datasets for Drought Monitoring in Chile. *Atmos. Res.* **2017**, *186*, 26–42. [[CrossRef](#)]
11. Zhong, R.; Chen, X.; Lai, C.; Wang, Z.; Lian, Y.; Yu, H.; Wu, X. Drought Monitoring Utility of Satellite-Based Precipitation Products across Mainland China. *J. Hydrol.* **2019**, *568*, 343–359. [[CrossRef](#)]
12. Rhee, J.; Im, J. Meteorological Drought Forecasting for Ungauged Areas Based on Machine Learning: Using Long-Range Climate Forecast and Remote Sensing Data. *Agric. For. Meteorol.* **2017**, *237–238*, 105–122. [[CrossRef](#)]
13. Park, S.; Im, J.; Han, D.; Rhee, J. Short-Term Forecasting of Satellite-Based Drought Indices Using Their Temporal Patterns and Numerical Model Output. *Remote Sens.* **2020**, *12*, 3499. [[CrossRef](#)]

14. Skinner, J.C.; Bellerby, J.T.; Greatrex, H.; Grimes, D.F.D. Hydrological Modelling Using Ensemble Satellite Rainfall Estimates in a Sparsely Gauged River Basin: The Need for Whole-Ensemble Calibration. *J. Hydrol.* **2015**, *522*, 110–122. [[CrossRef](#)]
15. Gilewski, P.; Nawalany, M. Inter-Comparison of Rain-Gauge, Radar, and Satellite (IMERG GPM) Precipitation Estimates Performance for Rainfall-Runoff Modeling in a Mountainous Catchment in Poland. *Water* **2018**, *10*, 1665. [[CrossRef](#)]
16. Ma, Q.; Xiong, L.; Liu, D.; Xu, C.Y.; Guo, S. Evaluating the Temporal Dynamics of Uncertainty Contribution from Satellite Precipitation Input in Rainfall-Runoff Modeling Using the Variance Decomposition Method. *Remote Sens.* **2018**, *10*, 1876. [[CrossRef](#)]
17. Kim, J.P.; Jung, I.W.; Park, K.W.; Yoon, S.K.; Lee, D. Hydrological Utility and Uncertainty of Multi-Satellite Precipitation Products in the Mountainous Region of South Korea. *Remote Sens.* **2016**, *8*, 608. [[CrossRef](#)]
18. Ferraro, R.R.; Peters-lidard, C.D.; Hernandez, C.; Turk, F.J.; Aires, F.; Prigent, C.; Lin, X.; Boukabara, S.; Furuzawa, F.A.; Gopalan, K.; et al. An Evaluation of Microwave Land Surface Emissivities Over the Continental United States to Benefit GPM-Era Precipitation Algorithms. *IEEE Trans. Geosci. Remote Sens.* **2012**, *51*, 378–398. [[CrossRef](#)]
19. Yong, B.; Ren, L.L.; Hong, Y.; Wang, J.H.; Gourley, J.J.; Jiang, S.H.; Chen, X.; Wang, W. Hydrologic Evaluation of Multisatellite Precipitation Analysis Standard Precipitation Products in Basins beyond Its Inclined Latitude Band: A Case Study in Laohahe Basin, China. *Water Resour. Res.* **2010**, *46*, 759–768. [[CrossRef](#)]
20. Hasenauer, S.; Kidd, R.; Dorigo, W.; Wagner, W.; Levizzani, V. Journal of Geophysical Research: Atmospheres Rainfall from Satellite Soil Moisture Data. *J. Geophys. Res. Atmos.* **2014**, *119*, 5128–5141. [[CrossRef](#)]
21. Oliveira, R.; Maggioni, V.; Vila, D.; Morales, C. Characteristics and Diurnal Cycle of GPM Rainfall Estimates over the Central Amazon Region. *Remote Sens.* **2016**, *8*, 544. [[CrossRef](#)]
22. Huffman, G.J.; Gsfc, N.; Bolvin, D.T.; Braithwaite, D.; Hsu, K.; Joyce, R.; Kidd, C.; Nelkin, E.J.; Sorooshian, S.; Tan, J.; et al. *Algorithm Theoretical Basis Document (ATBD) NASA Global Precipitation Measurement (GPM) Integrated Multi-SatellitE Retrievals for GPM (IMERG)*; NASA: Washington, DC, USA, 2017.
23. Sharif, H.O.; Al-Zahrani, M.; El Hassan, A. Physically, Fully-Distributed Hydrologic Simulations Driven by GPM Satellite Rainfall over an Urbanizing Arid Catchment in Saudi Arabia. *Water* **2017**, *9*, 163. [[CrossRef](#)]
24. Hou, A.Y.; Kakar, R.K.; Neeck, S.; Azarbarzin, A.A.; Kummerow, C.D.; Kojima, M.; Oki, R.; Nakamura, K.; Iguchi, T. The global precipitation measurement mission. *Bull. Am. Meteorol. Soc.* **2014**, *95*, 701–722. [[CrossRef](#)]
25. Collischonn, W. Método de Combinação de Dados de Precipitação Estimados Por Satélite e Medidos Em Pluviômetros Para a Modelagem Hidrológica [Merging Rainfall Gauges and Satellite Rainfall Data for Hydrology Modeling]. *Rev. Bras. Recur. Hídricos* **2015**, *20*, 202–217.
26. Ma, Y.; Tang, G.; Long, D.; Yong, B.; Zhong, L.; Wan, W.; Hong, Y. Similarity and Error Intercomparison of the GPM and Its Predecessor-TRMM Multisatellite Precipitation Analysis Using the Best Available Hourly Gauge Network over the Tibetan Plateau. *Remote Sens.* **2016**, *8*, 569. [[CrossRef](#)]
27. Ma, Y.; Zhang, Y.; Yang, D.; Farhan, S. bin Precipitation Bias Variability versus Various Gauges under Different Climatic Conditions over the Third Pole Environment (TPE) Region. *Int. J. Climatol.* **2015**, *35*, 1201–1211. [[CrossRef](#)]
28. Tesfagiorgis, K.; Mahani, S.E.; Krakauer, N.Y.; Khanbilvardi, R. Bias Correction of Satellite Rainfall Estimates Using a Radar-Gauge Product—a Case Study in Oklahoma (USA). *Hydrol. Earth Syst. Sci.* **2011**, *15*, 2631–2647. [[CrossRef](#)]
29. Melo, D.d.C.D.; Xavier, A.C.; Bianchi, T.; Oliveira, P.T.S.; Scanlon, B.R.; Lucas, M.C.; Wendland, E. Performance Evaluation of Rainfall Estimates by TRMM Multi-Satellite Precipitation Analysis 3B42V6 and V7 over Brazil. *J. Geophys. Res.* **2015**, *120*, 9426–9436. [[CrossRef](#)]
30. Pradhan, R.K.; Markonis, Y.; Vargas Godoy, M.R.; Villalba-Pradas, A.; Andreadis, K.M.; Nikolopoulos, E.I.; Papalexiou, S.M.; Rahim, A.; Tapiador, F.J.; Hanel, M. Review of GPM IMERG Performance: A Global Perspective. *Remote Sens. Environ.* **2021**, *268*, 112754. [[CrossRef](#)]
31. Prakash, S. Performance Assessment of CHIRPS, MSWEP, SM2RAIN-CCI, and TMPA Precipitation Products across India. *J. Hydrol.* **2019**, *571*, 50–59. [[CrossRef](#)]
32. Ramadhan, R.; Yusnaini, H.; Marzuki, M.; Muharsyah, R.; Suryanto, W.; Sholihun, S.; Vonnisa, M.; Harmadi, H.; Ningsih, A.P.; Battaglia, A.; et al. Evaluation of GPM IMERG Performance Using Gauge Data over Indonesian Maritime Continent at Different Time Scales. *Remote Sens.* **2022**, *14*, 1172. [[CrossRef](#)]
33. Yu, C.; Hu, D.; Liu, M.; Wang, S.; Di, Y. Spatio-Temporal Accuracy Evaluation of Three High-Resolution Satellite Precipitation Products in China Area. *Atmospheric Res.* **2020**, *241*, 104952. [[CrossRef](#)]
34. Derin, Y.; Anagnostou, E.; Berne, A.; Borga, M.; Boudevillain, B.; Buytaert, W.; Chang, C.H.; Chen, H.; Delrieu, G.; Hsu, Y.C.; et al. Evaluation of GPM-Era Global Satellite Precipitation Products over Multiple Complex Terrain Regions. *Remote Sens.* **2019**, *11*, 2936. [[CrossRef](#)]
35. de Moraes, R.B.F.; Gonçalves, F.V. Validation of Trmm Data in the Geographical Regions of Brazil. *Rev. Bras. Recur. Hídric.* **2021**, *26*, e36. [[CrossRef](#)]
36. Tang, G.; Ma, Y.; Long, D.; Zhong, L.; Hong, Y. Evaluation of GPM Day-1 IMERG and TMPA Version-7 Legacy Products over Mainland China at Multiple Spatiotemporal Scales. *J. Hydrol.* **2016**, *533*, 152–167. [[CrossRef](#)]
37. Sharifi, E.; Steinacker, R.; Saghafian, B. Assessment of GPM-IMERG and Other Precipitation Products against Gauge Data under Different Topographic and Climatic Conditions in Iran: Preliminary Results. *Remote Sens.* **2016**, *8*, 135. [[CrossRef](#)]

38. de Paes, R.P.; Costa, V.A.F.; Fernandes, W.D.S. Effects of Small Hydropower Plants in Cascade Arrangement on the Discharge Cyclic Patterns. *Rev. Bras. Recur. Hidr.* **2019**, *24*, e33. [[CrossRef](#)]
39. PRODUCT 5: State Water Resources Plan Final Review; Goiás, Brazil, 2015. Available online: [https://www.meioambiente.gov.br/images/imagens\\_migradas/upload/arquivos/2016-01/p05\\_plano\\_estadual\\_de\\_recursos\\_hidricos\\_revfinal2016.pdf](https://www.meioambiente.gov.br/images/imagens_migradas/upload/arquivos/2016-01/p05_plano_estadual_de_recursos_hidricos_revfinal2016.pdf) (accessed on 7 June 2022).
40. Santos, F.P.; Bayer, M.; Carvalho, T.M. Compartimentação Pedológica da Bacia do Rio dos Bois, Municípios de Cezarina, Varjão, Guapó Ee Palmeiras de Goiás (Go), e Sua Relação com a Suscetibilidade e Risco à Erosão Laminar. *J. Exp. Psychol. Gen.* **2008**, *136*, 23–42.
41. Package, T.; Hydrology, T.; Forecasting, C. Package ‘Hyfo’. 2018. Available online: <https://cran.r-project.org/web/packages/hyfo/index.html> (accessed on 7 June 2022).
42. Miró, J.J.; Caselles, V.; Estrela, M.J. Multiple Imputation of Rainfall Missing Data in the Iberian Mediterranean Context. *Atmos. Res.* **2017**, *197*, 313–330. [[CrossRef](#)]
43. Borga, M.; Vizzaccaro, A. On the Interpolation of Hydrologic Variables: Formal Equivalence of Multiquadratic Surface Fitting and Kriging. *J. Hydrol.* **1997**, *195*, 160–171. [[CrossRef](#)]
44. Plouffe, C.C.F.; Robertson, C.; Chandrapala, L. Comparing Interpolation Techniques for Monthly Rainfall Mapping Using Multiple Evaluation Criteria and Auxiliary Data Sources: A Case Study of Sri Lanka. *Environ. Model. Softw.* **2015**, *67*, 57–71. [[CrossRef](#)]
45. Biondi, D.; Freni, G.; Iacobellis, V.; Mascaro, G.; Montanari, A. Validation of Hydrological Models: Conceptual Basis, Methodological Approaches and a Proposal for a Code of Practice. *Phys. Chem. Earth* **2012**, *42–44*, 70–76. [[CrossRef](#)]
46. Schaepli, B.; Gupta, H.V. Do Nash Values Have Value? *Hydrol. Process.* **2007**, *21*, 2075–2080. [[CrossRef](#)]
47. Costa, V.; Fernandes, W.; Starick, Â. Identifying Regional Models for Flow Duration Curves with Evolutionary Polynomial Regression: Application for Intermittent Streams. *J. Hydrol. Eng.* **2020**, *25*, 04019059. [[CrossRef](#)]
48. Mahmud, M.R.; Hashim, M.; Nadzri, M.; Reba, M. How Effective Is the New Generation of GPM Satellite Precipitation in Characterizing the Rainfall Variability over Malaysia ? *Asia Pac. J. Atmos. Sci.* **2017**, *53*, 375–384. [[CrossRef](#)]